EFFECT OF STRESS CONCENTRATION ON LAMINATED PLATES

A. S. Sayyad *

Department of Civil Engineering
SRES'S College of Engineering
Kopargaon-423601, India

Y. M. Ghugal

Department of Applied Mechanics
Government Engineering College
Aurangabad-431005, India

ABSTRACT

This paper deals with the problem of stress distribution in orthotropic and laminated plates subjected to central concentrated load. An equivalent single layer trigonometric shear deformation theory taking into account transverse shear deformation effect as well as transverse normal strain effect is used to obtain inplane normal and transverse shear stresses through the thickness of plate. Governing equations and boundary conditions of the theory are obtained using the principle of virtual work. A simply supported plate with central concentrated load is considered for the numerical analysis. Anomalous behavior of inplane normal and transverse shear stresses is observed due to effect of stress concentration compared to classical plate theory and first order shear deformation theory.

Keywords: Transverse shear, Transverse normal strain, Static flexure, Laminated plates, Concentrated loads, Stress concentration.

1. INTRODUCTION

Advances in the technology of composite materials has led to the use of composite plates as structural components in various engineering applications due to superior mechanical properties of these materials. However, shear deformation effects become more pronounced in such structures due to low transverse shear moduli as compared to inplane tensile moduli, when subjected to transverse loads. This necessitates the accurate structural analysis of composite plates. The effect of local stress concentration is more pronounced in laminated composites due to built in boundary conditions or concentrated loading conditions.

Since the transverse shear deformation is neglected in classical plate theory [1,2], it can not be applied to thick plate wherein shear deformation effects are more significant. First order shear deformation theory is considered as an improvement over classical plate theory. Reissner [3,4] was the first to provide consistent stress-based plate theory which incorporates the effect of shear deformation whereas Mindlin [5] has developed displacement based first order shear deformation theory. In these theories, the transverse shear strain distribution is assumed to be constant through the plate thickness and therefore problem dependent shear correction factor is required to account for the strain energy of shear deformation.

The limitations of classical, first and second order shear deformation theories stimulated the development of higher order or equivalent shear deformation theories to avoid the use of shear correction factors, to include effect of cross sectional warping and to get the realistic variation of the transverse shear strains and stresses through the thickness of plate. It was observed that most of the displacement models utilize some simplification of the generalized displacement function given by Lo *et al*. [6-8]. Reddy [9,10] used displacement function which has same number of unknowns as that of Mindlin type of displacement function, but the displacement function satisfies transverse shear stress condition at the top and bottom surfaces of the plate.

Kant [11] presented a third-order refined shear deformation theory for analysis of thick elastic plates which gives rise to a twelfth order governing differential equation system. Savitri and Varadan [12] have carried out analysis of laminated plate subjected to central concentrated load but not assess the effect of local stress concentration.

Comprehensive reviews of these theories have been given by Noor and Burton [13]. A recent review paper with future direction is presented by Ghugal and Shimpi [14].

Levy [15] has developed a refined theory for thick

* Corresponding author (attu_sayyad@yahoo.co.in)

DOI : 10.1017/jmech.2012.131
Copyright © 2013 The Society of Theoretical and Applied Mechanics, R.O.C.
https://doi.org/10.1017/jmech.2012.131 Published online by Cambridge University Press

isotropic plate for the first time using sinusoidal functions interms of thickness coordinate in the displacement field. Stein [16], Stein *et al.* [17,18], also proposed such theory and applied to isotropic plates in the modified form. In this paper trigonometric shear deformation theory is presented and applied to composite plates subjected to central concentrate load. The results for this loading case are rarely available in the literature. The effect of local stress concentration due to concentrated load is effectively assess by present theory which was not been assessed by the other researcher. The results obtained for stresses are compared with other refined theories to demonstrate the validity of the theory.

1.1 Plate Under Consideration

Consider a plate made up of orthotropic material of length a, width b, and thickness h. The plate occupies (in o– x – y – z right-handed Cartesian coordinate system) a region:

$$0 \le x \le a \ ; \ 0 \le y \le b \ ; \ -h/2 \le z \le h/2 \tag{1}$$

1.2 The Displacement Field

The displacement field of the present plate theory including mid-plane displacement components is written as follows:

$$\begin{aligned} u(x, y, z) &= u_0(x, y) - z\frac{\partial w}{\partial x} + \frac{h}{\pi}\sin\frac{\pi z}{h}\,\phi(x, y) \\ v(x, y, z) &= v_0(x, y) - z\frac{\partial w}{\partial y} + \frac{h}{\pi}\sin\frac{\pi z}{h}\,\psi(x, y) \\ w(x, y, z) &= w(x, y) + \frac{h}{\pi}\cos\frac{\pi z}{h}\,\xi(x, y) \end{aligned} \tag{2}$$

where u and v are the inplane displacements in x- and y-directions respectively and w is transverse displacement in z- direction. u_0 and v_0 are the mid-plane displacements and are the functions of x and y. The sinusoidal function is assigned according to the shear stress distribution through the thickness of the plate. The functions $\phi(x, y)$, $\psi(x, y)$ and $\xi(x, y)$ represent rotations of the plate at neutral plane, which are unknown functions to be determined.

1.3 Superiority of the Present Theory

The proposed theory is a displacement-based refined equivalent single layer theory, and refined shear deformation theories are known to be successful technique for improving the accuracy of displacement and stresses [19]. The kinematics of the present theory is much richer than those of the higher order shear deformation theories available in the literature, because if the trigonometric term interms of thickness coordinate is expanded in power series, the kinematics of higher order theories are implicitly taken into account to good deal of extent. Also, it needs to be noted that every additional power of thickness coordinate in the displacement field of other higher-order theories of Lo *et al.* [6,7] type not only introduces additional unknown variables in those theories but these variables are also difficult to interpret physically [20]. Thus use of the sine term in the thickness coordinate enhances the richness of the theory, and also results in the reduction of the number of unknown variables as compared to other theories [21,22] without loss of physics of the problem in modeling. The theory gives the realistic variation of transverse shear stress through the thickness of plate which is governed by a cosine-law distribution and satisfies the shear stress free boundary conditions on the top and bottom surfaces of the plate. The theory obviates the need of a shear correction factor due to the realistic variation of transverse shear stress. Thus, the displacement field chosen is superior to those of others. The boundary value problem of the theory is derived using principle of virtual work; hence the present theory is variationally consistent.

Normal and shear strains are obtained using strain-displacement relationship as follows:

Normal Strains:

$$\begin{aligned} \varepsilon_x &= \frac{\partial u}{\partial x} = \frac{\partial u_0}{\partial x} - z\frac{\partial^2 w}{\partial x^2} + \frac{h}{\pi}\sin\frac{\pi z}{h}\frac{\partial \phi}{\partial x} \\ \varepsilon_y &= \frac{\partial v}{\partial y} = \frac{\partial v_0}{\partial y} - z\frac{\partial^2 w}{\partial y^2} + \frac{h}{\pi}\sin\frac{\pi z}{h}\frac{\partial \psi}{\partial y} \\ \varepsilon_z &= \frac{\partial w}{\partial z} = -\xi\sin\frac{\pi z}{h} \end{aligned} \tag{3}$$

Shear Strains:

$$\begin{aligned} \gamma_{xy} &= \frac{\partial u}{\partial y} + \frac{\partial v}{\partial x} = \frac{\partial u_0}{\partial y} + \frac{\partial v_0}{\partial x} - 2z\frac{\partial^2 w}{\partial x \partial y} \\ &\quad + \frac{h}{\pi}\sin\frac{\pi z}{h}\left(\frac{\partial \phi}{\partial y} + \frac{\partial \psi}{\partial x}\right) \\ \gamma_{xz} &= \frac{\partial u}{\partial z} + \frac{\partial w}{\partial x} = \cos\frac{\pi z}{h}\left(\frac{h}{\pi}\frac{\partial \xi}{\partial x} + \phi\right) \\ \gamma_{yz} &= \frac{\partial v}{\partial z} + \frac{\partial w}{\partial y} = \cos\frac{\pi z}{h}\left(\frac{h}{\pi}\frac{\partial \xi}{\partial y} + \psi\right) \end{aligned} \tag{4}$$

The stress strain relationship for the plate of constant thickness h and composed of thin layers of orthotropic materials given by Jones [23] can be written as:

$$\begin{aligned} \sigma_x^k &= \bar{Q}_{11}^k\,\varepsilon_x + \bar{Q}_{12}^k\,\varepsilon_y + \bar{Q}_{13}^k\,\varepsilon_z \\ \sigma_y^k &= \bar{Q}_{12}^k\,\varepsilon_x + \bar{Q}_{22}^k\,\varepsilon_y + \bar{Q}_{23}^k\,\varepsilon_z \\ \sigma_z^k &= \bar{Q}_{13}^k\,\varepsilon_x + \bar{Q}_{23}^k\,\varepsilon_y + \bar{Q}_{33}^k\,\varepsilon_z \\ \tau_{xy}^k &= \bar{Q}_{66}^k\,\gamma_{xy}\,;\,\tau_{zx}^k = \bar{Q}_{55}^k\,\gamma_{zx}\,;\,\tau_{yz}^k = \bar{Q}_{44}^k\,\gamma_{yz} \end{aligned} \tag{5}$$

where $\bar{Q}_{ij}^k$ are the reduced plate stiffnesses coefficients as below:

https://doi.org/10.1017/jmech.2012.131 Published online by Cambridge University Press

$$\Delta = \begin{pmatrix} 1-\mu_{12}\,\mu_{21}-\mu_{23}\,\mu_{32} \\ -\mu_{31}\,\mu_{13}-2\,\mu_{21}\,\mu_{32}\,\mu_{13} \end{pmatrix}$$

$$\bar{Q}_{11}=\frac{E_1\,(1-\mu_{23}\,\mu_{32})}{\Delta}\;;\;\bar{Q}_{12}=\frac{E_1\,(\mu_{21}-\mu_{31}\,\mu_{23})}{\Delta}\;;$$

$$\bar{Q}_{13}=\frac{E_1\,(\mu_{31}-\mu_{21}\,\mu_{32})}{\Delta}\;;\;\bar{Q}_{22}=\frac{E_2\,(1-\mu_{13}\,\mu_{31})}{\Delta}\;;$$

$$\bar{Q}_{23}=\frac{E_2\,(\mu_{32}-\mu_{12}\,\mu_{31})}{\Delta}\;;\;\bar{Q}_{33}=\frac{E_3\,(1-\mu_{12}\,\mu_{21})}{\Delta}\;;$$

$$\bar{Q}_{66}=G_{12}\;;\quad \bar{Q}_{55}=G_{13}\;;\quad \bar{Q}_{44}=G_{23} \tag{6}$$

1.4 Governing Equations and Boundary Conditions

Using Eqs. (3) through (6) and principle of virtual work, variationally consistent differential equations and boundary conditions for the plate under consideration are obtained. The principle of virtual work can be stated in analytical form for the plate as:

$$\int_{-h/2}^{h/2}\int_0^b\int_0^a \begin{bmatrix} \sigma_x^k\,\delta\varepsilon_x+\sigma_y^k\,\delta\varepsilon_y+\sigma_z^k\,\delta\varepsilon_z+ \\ \tau_{xy}^k\,\delta\gamma_{xy}+\tau_{zy}^k\,\delta\gamma_{zy}+\tau_{zx}^k\,\delta\gamma_{zx} \end{bmatrix} dx\,dy\,dz$$

$$-\int_0^b\int_0^a q(x,y)\;\delta w\,dx\,dy=0 \tag{7}$$

Integrating the Eq. (7) by parts and collecting the coefficients of δu_0, δv_0, δw, $\delta\phi$, $\delta\psi$ and $\delta\xi$, we obtain the governing equations and the associated boundary conditions of the plate in terms of stress resultants and unknown variables appeared in the displacement field. The governing differential equations in-terms of stress resultants are as follows:

$$\frac{\partial N_x}{\partial x}+\frac{\partial N_{xy}}{\partial y}=0 \tag{8}$$

$$\frac{\partial N_{xy}}{\partial x}+\frac{\partial N_y}{\partial y}=0 \tag{9}$$

$$\frac{\partial^2 M_x}{\partial x^2}+2\frac{\partial^2 M_{xy}}{\partial x\partial y}+\frac{\partial^2 M_y}{\partial y^2}+q=0 \tag{10}$$

$$\frac{\partial M_x^s}{\partial x}+\frac{\partial M_{xy}^s}{\partial y}-V_{xz}^s=0 \tag{11}$$

$$\frac{\partial M_y^s}{\partial y}+\frac{\partial M_{xy}^s}{\partial x}-V_{yz}^s=0 \tag{12}$$

$$\frac{\partial V_{xz}^s}{\partial x}+\frac{\partial V_{yz}^s}{\partial y}-\frac{\pi}{h}V_{zz}^s=0 \tag{13}$$

The associated boundary conditions at $x = 0$ and $x = a$ obtained are of the following form:

$$N_x=0 \text{ or } u_0 \text{ is prescribed} \tag{14}$$

$$N_{xy}=0 \text{ or } v_0 \text{ is prescribed} \tag{15}$$

$$M_x=0 \text{ or } \frac{\partial w}{\partial x} \text{ is prescribed} \tag{16}$$

$$\frac{\partial M_x}{\partial x}+2\frac{\partial M_{xy}}{\partial y}=0 \text{ or } w \text{ is prescribed} \tag{17}$$

$$M_x^s=0 \text{ or } \phi \text{ is prescribed} \tag{18}$$

$$M_{xy}^s=0 \text{ or } \psi \text{ is prescribed} \tag{19}$$

$$V_{xz}^s=0 \text{ or } \xi \text{ is prescribed} \tag{20}$$

along $y = 0$ and $y = b$ edges, the boundary conditions are as follows:

$$N_{xy}=0 \text{ or } u_0 \text{ is prescribed} \tag{21}$$

$$N_y=0 \text{ or } v_0 \text{ is prescribed} \tag{22}$$

$$M_y=0 \text{ or } \frac{\partial w}{\partial y} \text{ is prescribed} \tag{23}$$

$$\frac{\partial M_y}{\partial y}+2\frac{\partial M_{xy}}{\partial x}=0 \text{ or } w \text{ is prescribed} \tag{24}$$

$$M_y^s=0 \text{ or } \psi \text{ is prescribed} \tag{25}$$

$$M_{xy}^s=0 \text{ or } \phi \text{ is prescribed} \tag{26}$$

$$V_{yz}^s=0 \text{ or } \xi \text{ is prescribed} \tag{27}$$

At corners of the plate, boundary condition is:

$$M_{xy}=0 \text{ or } w \text{ is prescribed} \tag{28}$$

The force and moment results appeared in governing equations [Eqs. (8) through (13)] and boundary conditions [Eqs. (14) through (28)] are as follows:

$$(N_x,\,N_y,\,N_{xy})=\int_{-h/2}^{h/2}(\sigma_x,\,\sigma_y,\,\tau_{xy})\,dz \tag{29}$$

$$(M_x,\,M_y,\,M_{xy})=\int_{-h/2}^{h/2}(\sigma_x,\,\sigma_y,\,\tau_{xy})\,z\,dz \tag{30}$$

$$(M_x^s,\,M_y^s,\,M_{xy}^s)=\int_{-h/2}^{h/2}(\sigma_x,\,\sigma_y,\,\tau_{xy})f(z)\;dz \tag{31}$$

$$(V_{xz}^s,\,V_{yz}^s)=\int_{-h/2}^{h/2}(\tau_{xz},\,\tau_{yz})f'(z)\;dz \tag{32}$$

$$V_{zz}^s=\int_{-h/2}^{h/2}\sigma_{zz}g'(z)\,dz \tag{33}$$

where N_x, N_y, N_{xy} are the force resultants analogous to classical plate theory, M_x, M_y, M_{xy} are the moment resultants or the stress couples analogous to classical plate theory, M_x^s, M_y^s, M_{xy}^s are refined moments or stress couples due to transverse shear deformation effects and V_{xz}^s, V_{yz}^s, V_{zz}^s are the transverse shear and

https://doi.org/10.1017/jmech.2012.131 Published online by Cambridge University Press

transverse normal stress resultants and $f(z) = h/\pi \sin \pi z/h$, $g(z) = h/\pi \cos \pi z/h$ and the prime $(\,)'$ indicates the differentiation of function with respect to z. The governing equations [Eqs. (8) through (13)] and associated boundary conditions [Eqs. (14) through (28)] in-terms of unknown variables (u_0, v_0, w, ϕ, ψ and ξ) in the displacement field are as follows:

$$
\begin{aligned}
&A_{11}\frac{\partial^2 u_0}{\partial x^2}+A_{66}\frac{\partial^2 u_0}{\partial y^2}+(A_{12}+A_{66})\frac{\partial^2 v_0}{\partial x\partial y}\\
&-B_{11}\frac{\partial^3 w}{\partial x^3}-(B_{12}+2B_{66})\frac{\partial^3 w}{\partial x\partial y^2}+As_{11}\frac{\partial^2 \phi}{\partial x^2}\\
&+As_{66}\frac{\partial^2 \phi}{\partial y^2}+(As_{12}+As_{66})\frac{\partial^2 \psi}{\partial x\partial y}\\
&-\frac{\pi}{h}As_{13}\frac{\partial \xi}{\partial x}=0
\end{aligned}
\tag{34}
$$

$$
\begin{aligned}
&(A_{12}+A_{66})\frac{\partial^2 u_0}{\partial x\partial y}+A_{66}\frac{\partial^2 v_0}{\partial x^2}+A_{22}\frac{\partial^2 v_0}{\partial y^2}\\
&-B_{22}\frac{\partial^3 w}{\partial y^3}-(B_{12}+2B_{66})\frac{\partial^3 w}{\partial x^2\partial y}\\
&+(As_{12}+As_{66})\frac{\partial^2 \phi}{\partial x\partial y}+As_{66}\frac{\partial^2 \psi}{\partial x^2}\\
&+As_{22}\frac{\partial^2 \psi}{\partial y^2}-\frac{\pi}{h}As_{23}\frac{\partial \xi}{\partial y}=0
\end{aligned}
\tag{35}
$$

$$
\begin{aligned}
&-B_{11}\frac{\partial^3 u_0}{\partial x^3}-(B_{12}+2B_{66})\frac{\partial^3 u_0}{\partial x\partial y^2}-B_{22}\frac{\partial^3 v_0}{\partial y^3}\\
&-(B_{12}+2B_{66})\frac{\partial^3 v_0}{\partial x^2\partial y}+D_{11}\frac{\partial^4 w}{\partial x^4}\\
&+2(D_{12}+2D_{66})\frac{\partial^4 w}{\partial x^2\partial y^2}+D_{22}\frac{\partial^4 w}{\partial y^4}-Bs_{11}\frac{\partial^3 \phi}{\partial x^3}\\
&-(Bs_{12}+2Bs_{66})\frac{\partial^3 \phi}{\partial x\partial y^2}-Bs_{22}\frac{\partial^3 \psi}{\partial y^3}\\
&-(Bs_{12}+2Bs_{66})\frac{\partial^3 \psi}{\partial x^2\partial y}\\
&+\frac{\pi}{h}\left(Bs_{13}\frac{\partial^2 \xi}{\partial x^2}+Bs_{23}\frac{\partial^2 \xi}{\partial y^2}\right)=q
\end{aligned}
\tag{36}
$$

$$
\begin{aligned}
&As_{11}\frac{\partial^2 u_0}{\partial x^2}+As_{66}\frac{\partial^2 u_0}{\partial y^2}+(As_{12}+As_{66})\frac{\partial^2 v_0}{\partial x\partial y}\\
&-Bs_{11}\frac{\partial^3 w}{\partial x^3}-(Bs_{12}+2Bs_{66})\frac{\partial^3 w}{\partial x\partial y^2}+Ass_{11}\frac{\partial^2 \phi}{\partial x^2}\\
&+Ass_{66}\frac{\partial^2 \phi}{\partial y^2}-Acc_{55}\phi+(Ass_{12}+Ass_{66})\frac{\partial^2 \psi}{\partial x\partial y}\\
&-\left(\frac{\pi}{h}Ass_{13}+\frac{h}{\pi}Acc_{55}\right)\frac{\partial \xi}{\partial x}=0
\end{aligned}
\tag{37}
$$

$$
\begin{aligned}
&(As_{12}+As_{66})\frac{\partial^2 u_0}{\partial x\partial y}+As_{66}\frac{\partial^2 v_0}{\partial x^2}+As_{22}\frac{\partial^2 v_0}{\partial y^2}\\
&-Bs_{22}\frac{\partial^3 w}{\partial y^3}-(Bs_{12}+2Bs_{66})\frac{\partial^3 w}{\partial x^2\partial y}\\
&+(Ass_{12}+Ass_{66})\frac{\partial^2 \phi}{\partial x\partial y}+Ass_{66}\frac{\partial^2 \psi}{\partial x^2}+Ass_{22}\frac{\partial^2 \psi}{\partial y^2}\\
&-Acc_{44}\psi-\left(\frac{\pi}{h}Ass_{23}+\frac{h}{\pi}Acc_{44}\right)\frac{\partial \xi}{\partial y}=0
\end{aligned}
\tag{38}
$$

$$
\begin{aligned}
&\frac{\pi}{h}As_{13}\frac{\partial u_0}{\partial x}+\frac{\pi}{h}As_{23}\frac{\partial v_0}{\partial y}-\frac{\pi}{h}Bs_{13}\frac{\partial^2 w}{\partial x^2}\\
&-\frac{\pi}{h}Bs_{23}\frac{\partial^2 w}{\partial y^2}+\left(\frac{\pi}{h}Ass_{13}+\frac{h}{\pi}Acc_{55}\right)\frac{\partial \phi}{\partial x}\\
&+\left(\frac{\pi}{h}Ass_{23}+\frac{h}{\pi}Acc_{44}\right)\frac{\partial \psi}{\partial y}-\frac{\pi^2}{h^2}Ass_{33}\xi\\
&+\frac{h^2}{\pi^2}Acc_{44}\frac{\partial^2 \xi}{\partial y^2}+\frac{h^2}{\pi^2}Acc_{55}\frac{\partial^2 \xi}{\partial x^2}=0
\end{aligned}
\tag{39}
$$

The associated boundary conditions are as follows:

On edges $x = 0$ and $x = a$, the following conditions hold:

$$
\begin{aligned}
&A_{11}\frac{\partial u_0}{\partial x}+A_{12}\frac{\partial v_0}{\partial y}-B_{11}\frac{\partial^2 w}{\partial x^2}-B_{12}\frac{\partial^2 w}{\partial y^2}\\
&+As_{11}\frac{\partial \phi}{\partial x}+As_{12}\frac{\partial \psi}{\partial y}-\frac{\pi}{h}As_{13}\xi=0\\
&\text{or } u_0 \text{ is prescribed}
\end{aligned}
\tag{40}
$$

$$
\begin{aligned}
&A_{66}\left(\frac{\partial u_0}{\partial y}+\frac{\partial v_0}{\partial x}\right)-2B_{66}\frac{\partial^2 w}{\partial x\partial y}+As_{66}\left(\frac{\partial \phi}{\partial y}+\frac{\partial \psi}{\partial x}\right)=0\\
&\text{or } v_0 \text{ is prescribed}
\end{aligned}
\tag{41}
$$

$$
\begin{aligned}
&B_{11}\frac{\partial^2 u_0}{\partial x^2}+2B_{66}\frac{\partial^2 u_0}{\partial y^2}+(B_{12}+2B_{66})\frac{\partial^2 v_0}{\partial x\partial y}-D_{11}\frac{\partial^3 w}{\partial x^3}\\
&-(D_{12}+4D_{66})\frac{\partial^3 w}{\partial x\partial y^2}+Bs_{11}\frac{\partial^2 \phi}{\partial x^2}+2Bs_{66}\frac{\partial^2 \phi}{\partial y^2}\\
&+(Bs_{12}+2Bs_{66})\frac{\partial^2 \psi}{\partial x\partial y}-\frac{\pi}{h}Bs_{13}\frac{\partial \xi}{\partial x}=0\\
&\text{or } w \text{ is prescribed}
\end{aligned}
\tag{42}
$$

$$
\begin{aligned}
&B_{11}\frac{\partial u_0}{\partial x}+B_{12}\frac{\partial v_0}{\partial y}-D_{11}\frac{\partial^2 w}{\partial x^2}-D_{12}\frac{\partial^2 w}{\partial y^2}\\
&+Bs_{11}\frac{\partial \phi}{\partial x}+Bs_{12}\frac{\partial \psi}{\partial y}-\frac{\pi}{h}Bs_{13}\,\xi=0\\
&\text{or } \frac{\partial w}{\partial x} \text{ is prescribed}
\end{aligned}
\tag{43}
$$

$$
\begin{aligned}
&As_{11}\frac{\partial u_0}{\partial x}+As_{12}\frac{\partial v_0}{\partial y}-Bs_{11}\frac{\partial^2 w}{\partial x^2}-Bs_{12}\frac{\partial^2 w}{\partial y^2}\\
&+Ass_{11}\frac{\partial \phi}{\partial x}+Ass_{12}\frac{\partial \psi}{\partial y}-\frac{\pi}{h}Ass_{13}\,\xi=0\\
&\text{or } \phi \text{ is prescribed}
\end{aligned}
\tag{44}
$$

https://doi.org/10.1017/jmech.2012.131 Published online by Cambridge University Press

$$As_{66}\left(\frac{\partial u_0}{\partial y}+\frac{\partial v_0}{\partial x}\right)-2Bs_{66}\frac{\partial^2 w}{\partial x\partial y}$$
$$+Ass_{66}\left(\frac{\partial \phi}{\partial y}+\frac{\partial \psi}{\partial x}\right)=0$$
or ψ is prescribed (45)

$$\frac{h}{\pi}Acc_{55}\,\phi+\frac{h^2}{\pi^2}Acc_{55}\frac{\partial \xi}{\partial x}=0$$
or ξ is prescribed (46)

On edges $y = 0$ and $y = b$, the following conditions hold:

$$A_{66}\left(\frac{\partial u_0}{\partial y}+\frac{\partial v_0}{\partial x}\right)-2B_{66}\frac{\partial^2 w}{\partial x\partial y}+As_{66}\left(\frac{\partial \phi}{\partial y}+\frac{\partial \psi}{\partial x}\right)=0$$
or u_0 is prescribed (47)

$$A_{12}\frac{\partial u_0}{\partial x}+A_{22}\frac{\partial v_0}{\partial y}-B_{12}\frac{\partial^2 w}{\partial x^2}-B_{22}\frac{\partial^2 w}{\partial y^2}$$
$$+As_{12}\frac{\partial \phi}{\partial x}+As_{22}\frac{\partial \psi}{\partial y}-\frac{\pi}{h}As_{23}\,\xi=0$$
or v_0 is prescribed (48)

$$(B_{12}+2B_{66})\frac{\partial^2 u_0}{\partial x\partial y}+2B_{66}\frac{\partial^2 v_0}{\partial x^2}+B_{22}\frac{\partial^2 v_0}{\partial y^2}-D_{22}\frac{\partial^3 w}{\partial y^3}$$
$$-(D_{12}+4D_{66})\frac{\partial^3 w}{\partial x^2\partial y}+(Bs_{12}+2Bs_{66})\frac{\partial^2 \phi}{\partial x\partial y}$$
$$+2Bs_{66}\frac{\partial^2 \psi}{\partial x^2}+Bs_{22}\frac{\partial^2 \psi}{\partial y^2}-\frac{\pi}{h}Bs_{23}\frac{\partial \xi}{\partial y}=0$$
or w is prescribed (49)

$$B_{12}\frac{\partial u_0}{\partial x}+B_{22}\frac{\partial v_0}{\partial y}-D_{12}\frac{\partial^2 w}{\partial x^2}-D_{22}\frac{\partial^2 w}{\partial y^2}$$
$$+Bs_{12}\frac{\partial \phi}{\partial x}+Bs_{22}\frac{\partial \psi}{\partial y}-\frac{\pi}{h}Bs_{23}\,\xi=0$$
or $\dfrac{\partial w}{\partial y}$ is prescribed (50)

$$As_{66}\left(\frac{\partial u_0}{\partial y}+\frac{\partial v_0}{\partial x}\right)-2Bs_{66}\frac{\partial^2 w}{\partial x\partial y}$$
$$+Ass_{66}\left(\frac{\partial \phi}{\partial y}+\frac{\partial \psi}{\partial x}\right)=0$$
or ϕ is prescribed (51)

$$As_{12}\frac{\partial u_0}{\partial x}+As_{22}\frac{\partial v_0}{\partial y}-Bs_{12}\frac{\partial^2 w}{\partial x^2}-Bs_{22}\frac{\partial^2 w}{\partial y^2}$$
$$+Ass_{12}\frac{\partial \phi}{\partial x}+Ass_{22}\frac{\partial \psi}{\partial y}-\frac{\pi}{h}Ass_{23}\,\xi=0$$
or ψ is prescribed (52)

$$\frac{h}{\pi}Acc_{44}\,\psi+\frac{h^2}{\pi^2}Acc_{44}\frac{\partial \xi}{\partial y}=0$$
or ξ is prescribed (53)

At corners $(x = 0, y = 0)$, $(x = 0, y = b)$, $(x = a, y = 0)$ and $(x = a, y = b)$ the following condition hold:

$$B_{66}\left(\frac{\partial u_0}{\partial y}+\frac{\partial v_0}{\partial x}\right)-2D_{66}\frac{\partial^2 w}{\partial x\partial y}+Bs_{66}\left(\frac{\partial \phi}{\partial y}+\frac{\partial \psi}{\partial x}\right)=0$$
or w is prescribed (54)

2. ILLUSTRATIVE EXAMPLES

In order to prove the efficacy of the present theory, a square laminated plate simply supported along all edges is considered. A plate is subjected to concentrated load P on top ($z = -h/2$) of plate acting in z –direction as shown in Fig. 1.

The magnitude of transverse load is given as:

$$q(x,\,y)=\sum_{m=1}^{\infty}\sum_{n=1}^{\infty}q_{mn}\sin\alpha x\,\sin\beta y \tag{55}$$

where $\alpha = m\pi/a$ and $\beta = n\pi/b$

The q_{mn} is the coefficients of Fourier expansion of concentrated load which is given as:

$$q_{mn}=\left(\frac{4P}{ab}\right)\sin\alpha\zeta\sin\beta\eta \tag{56}$$

where ζ and η represent distance of concentrated load from x and y axes respectively. In case of central concentrated load $\zeta = a/2$ and $\eta = b/2$. The following solution form for u_0, v_0, w, ϕ, ψ and ξ satisfies the governing Eqs. (34) through (39) and the boundary conditions given by Eqs. (40) through (54) perfectly.

$$u_0=\sum_{m=1}^{m=\infty}\sum_{n=1}^{n=\infty}u_{mn}\cos\alpha x\sin\beta y\;; \tag{57}$$

$$v_0=\sum_{m=1}^{m=\infty}\sum_{n=1}^{n=\infty}v_{mn}\sin\alpha x\cos\beta y\;; \tag{58}$$

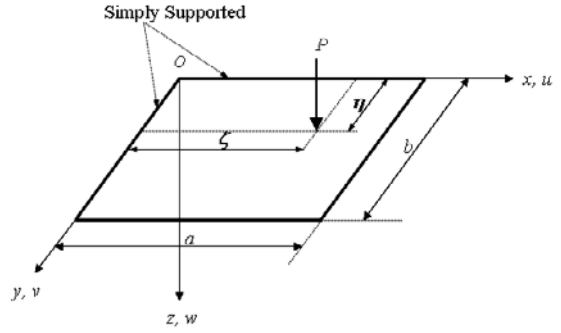


Fig. 1 Simply supported plate subjected to concentrated load

https://doi.org/10.1017/jmech.2012.131 Published online by Cambridge University Press

$$w=\sum_{m=1}^{m=\infty}\sum_{n=1}^{n=\infty} w_{mn}\sin\alpha x\sin\beta y\ ; \tag{59}$$

$$\phi=\sum_{m=1}^{m=\infty}\sum_{n=1}^{n=\infty} \phi_{mn}\cos\alpha x\sin\beta y\ ; \tag{60}$$

$$\psi=\sum_{m=1}^{m=\infty}\sum_{n=1}^{n=\infty} \psi_{mn}\sin\alpha x\cos\beta y\ ; \tag{61}$$

$$\xi=\sum_{m=1}^{m=\infty}\sum_{n=1}^{n=\infty} \xi_{mn}\sin\alpha x\sin\beta y \tag{62}$$

where u_{mn}, v_{mn}, w_{mn}, ϕ_{mn}, ψ_{mn} and ξ_{mn} are the unknown coefficients of the respective Fourier expansions and m, n are positive integers. Substituting this form of solution and the load $q(x, y)$ from Eq. (55) into the governing equations [Eqs. (34) through (39)] yields the six algebraic simultaneous equations which are expressed in the following matrix form:

$$\begin{bmatrix} K_{11} & K_{12} & K_{13} & K_{14} & K_{15} & K_{16} \\ K_{12} & K_{22} & K_{23} & K_{24} & K_{25} & K_{26} \\ K_{13} & K_{23} & K_{33} & K_{34} & K_{35} & K_{36} \\ K_{14} & K_{24} & K_{34} & K_{44} & K_{45} & K_{46} \\ K_{15} & K_{25} & K_{35} & K_{45} & K_{55} & K_{66} \\ K_{16} & K_{26} & K_{36} & K_{46} & K_{56} & K_{66} \end{bmatrix} \begin{Bmatrix} u_{mn} \\ v_{mn} \\ w_{mn} \\ \phi_{mn} \\ \psi_{mn} \\ \xi_{mn} \end{Bmatrix} = \begin{bmatrix} 0 \\ 0 \\ q_{mn} \\ 0 \\ 0 \\ 0 \end{bmatrix} \tag{63}$$

where, elements of stiffness matrix (K_{ij}) are given in Appendix. Solving above equations the unknowns u_{mn}, v_{mn}, w_{mn}, ϕ_{mn}, ψ_{mn} and ξ_{mn} can be readily determined as given below:

$$\begin{aligned} u_{mn} &= \bar{u}\, q_{mn}\ ; \quad & v_{mn} &= \bar{v}\, q_{mn} \\ w_{mn} &= \bar{w} q_{mn}\ ; \quad & \phi_{mn} &= \bar{\phi}\, q_{mn} \\ \psi_{mn} &= \bar{\psi}\, q_{mn}\ ; \quad & \xi_{mn} &= \bar{\xi}\, q_{mn} \end{aligned} \tag{64}$$

where, values of $\bar{u}, \bar{v}, \bar{w}, \bar{\phi}, \bar{\psi}$ and $\bar{\xi}$ are given in Appendix. Substitution of these unknowns into Eqs. (57) through (62) leads to the following equations.

$$u_0 = \bar{u}\ \cos\alpha x\ \sin\beta y\ q_{mn} \tag{65}$$

$$v_0 = \bar{v}\ \sin\alpha x\ \cos\beta y\ q_{mn} \tag{66}$$

$$w = \bar{w}\ \sin\alpha x\ \sin\beta y\ q_{mn} \tag{67}$$

$$\phi = \bar{\phi}\ \cos\alpha x\ \sin\beta y\ q_{mn} \tag{68}$$

$$\psi = \bar{\psi}\ \sin\alpha x\ \cos\beta y\ q_{mn} \tag{69}$$

$$\xi = \bar{\xi}\ \sin\alpha x\ \sin\beta y\ q_{mn} \tag{70}$$

2.1 Evaluation of Inplane Normal Stresses

Having obtained values of displacement variables [Eqs. (65) through (70)], one can then calculate all the displacement and stress components within the plate using displacement field [Eq. (2)] and stress-strain relationships [Eq. (5)]. The expressions obtained for inplane normal stresses are given in Eqs. (71) and (72).

$$\begin{aligned} \sigma_x^k = \Big[& -\bar{Q}_{11}^k\,\alpha\,\bar{u} + \bar{Q}_{11}^k\, z\alpha^2\bar{w} - \bar{Q}_{11}^k f(z)\,\alpha\,\bar{\phi} \\ & - \bar{Q}_{12}^k\,\beta\,\bar{v} + \bar{Q}_{12}^k\, z\beta^2\bar{w} - \bar{Q}_{12}^k f(z)\,\beta\,\bar{\psi} \\ & + \bar{Q}_{13}^k g'(z)\bar{\xi}\Big]\, q_{mn}\sin\alpha x\sin\beta y \end{aligned} \tag{71}$$

$$\begin{aligned} \sigma_y^k = \Big[& -\bar{Q}_{12}^k\,\alpha\,\bar{u} + \bar{Q}_{12}^k\, z\alpha^2\bar{w} - \bar{Q}_{12}^k f(z)\,\alpha\,\bar{\phi} \\ & - \bar{Q}_{22}^k\,\beta\,\bar{v} + \bar{Q}_{22}^k\, z\beta^2\bar{w} - \bar{Q}_{22}^k f(z)\,\beta\,\bar{\psi} \\ & + \bar{Q}_{23}^k g'(z)\bar{\xi}\Big]\, q_{mn}\sin\alpha x\sin\beta y \end{aligned} \tag{72}$$

2.2 Evaluation of Inplane shear Stress

Using Eqs. (65) through (70) the inplane shear stress is obtained from Eq. (5) as follows:

$$\begin{aligned} \tau_{xy}^k = \bar{Q}_{66}^k \Big[& \beta\bar{u} + \alpha\bar{v} - 2z\alpha\beta\bar{w} + f(z)\,\beta\bar{\phi} \\ & + f(z)\,\alpha\bar{\psi}\Big]\, q_{mn}\cos\alpha x\cos\beta y \end{aligned} \tag{73}$$

2.3 Evaluation of Transverse Shear Stresses

Transverse shear stresses can be calculated by using two approaches

Using Constitutive Relations (CR Approach): Constitutive relations are used in this approach. CR approach gives a discontinuity of stresses at interface in case of laminated plates; cause by mismatch in material properties of adjacent layers and thus violates the equilibrium conditions. This is not acceptable from physical point of view.

Using Equilibrium Equation (EE Approach): In this approach the transverse stresses are obtained by integrating the equilibrium equation with respect to thickness direction. EE approach ascertains the continuity of the stresses at interface.

The expressions obtained for transverse shear stresses using constitutive relations [Eq. (5)] are given in Eqs. (74) and (75).

$$\tau_{zx}^k = \bar{Q}_{55}^k\left[f'(z)\left(\frac{h}{\pi}\alpha\,\bar{\xi} + \bar{\phi}\right)\right] q_{mn}\cos\alpha x\sin\beta y \tag{74}$$

$$\tau_{yz}^k = \bar{Q}_{44}^k\left[f''(z)\left(\frac{h}{\pi}\beta\,\bar{\xi} + \bar{\psi}\right)\right] q_{mn}\sin\alpha x\cos\beta y \tag{75}$$

Transverse shear stresses are also obtained by integrating equations of equilibrium of theory of elasticity as follows:

$$\tau_{zx}^k = \int_{-h/2}^{z_k}\left(\frac{\partial\sigma_x}{\partial x} + \frac{\partial\tau_{xy}}{\partial y}\right) dz \tag{76}$$

$$\tau_{yz}^k = \int_{-h/2}^{z_k}\left(\frac{\partial\sigma_y}{\partial y} + \frac{\partial\tau_{xy}}{\partial x}\right) dz \tag{77}$$

The following lamina material properties given by Pagano [24] for plates in the above examples are used.

https://doi.org/10.1017/jmech.2012.131 Published online by Cambridge University Press

$$\frac{E_1}{E_2}=25\ ,\quad \frac{E_3}{E_2}=1\ ,\quad \frac{G_{12}}{E_2}=\frac{G_{13}}{E_2}=0.5\ ,\quad \frac{G_{23}}{E_2}=0.2\ ,$$
$$\mu_{12}=\mu_{13}=\mu_{23}=0.25 \qquad (78)$$

3. NUMERICAL RESULTS

The results are obtained for different aspect ratios ($S = a / h$) of plate are presented in Tables 1 through 9. Because of unavailability of exact solution for the loading case considered, the results from classical plate theory (CPT), first order shear deformation theory (FSDT) and higher order shear deformation theory of Reddy (HSDT) are generated for the purpose of comparison of results obtained by present theory (TSDT). The results obtained for inplane normal and transverse shear stresses are presented in the following non-dimensional form.

4. DISCUSSION OF RESULTS

From the numerical results (Tables 1 through 9) and stress distributions (Figs. 2 through 12) following observations are made.

1. Inplane Normal Stresses ($\bar{\sigma}_x$ and $\bar{\sigma}_y$):

The inplane normal stresses ($\bar{\sigma}_x$ and $\bar{\sigma}_y$) obtained by present theory are compared with those of other refined shear deformation theories for orthotropic plate in Table 1. It observed from these results that the maximum inplane normal stresses at the top and bottom surfaces of the plate obtained by present theory (TSDT) and theory of Reddy (HSDT) are higher than the one given by classical plate theory (CPT) and first order shear deformation theory (FSDT) due to effect of local stress concentration. Figure 2 shows the through thickness distribution of inplane normal stress $\bar{\sigma}_x$ in orthotropic plate for aspect ratio 4. Stress distribution shown in Fig. 2 by present theory and theory of Reddy is non-linear through the thickness of plate and deviates considerably from the one given by classical plate theory and first order shear deformation theory. This indicates that present theory is capable of predicting the effect of stress concentration and transverse shear deformation. Comparison of inplane normal stresses for two layered anti-symmetric ($0^0/90^0$) laminated plates is presented in Table 4. Examination of Table 4 reveals that the maximum values of inplane normal stresses $\bar{\sigma}_x$ and $\bar{\sigma}_y$ obtained by present theory and other theories are identical for both aspect ratios. The inplane normal stress $\bar{\sigma}_x$ is maximum at top (0^0 layer) and minimum at bottom (90^0 layer). Through thickness distribution of inplane normal stress $\bar{\sigma}_x$ in ($0^0/90^0$) laminated plate for aspect ratio 4 is shown in Fig. 5. From this distribution it is observed that the inplane normal stress changes its sign in both layers due

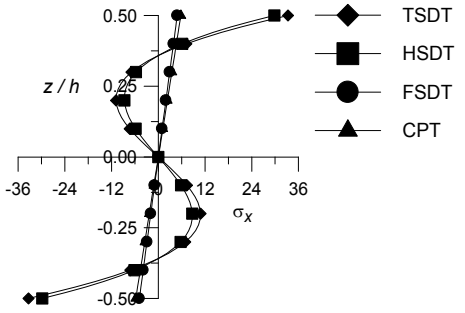


Fig. 2 Through thickness distribution of inplane normal stress ($\bar{\sigma}_x$) in orthotropic plate for aspect ratio 4

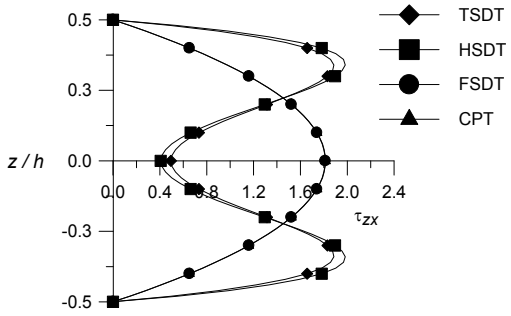


Fig. 3 Through thickness distribution of transverse shear stress ($\bar{\tau}_{zx}$) in orthotropic plate for aspect ratio 4 using equations of equilibrium

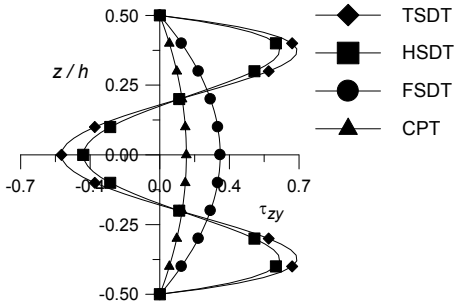


Fig. 4 Through thickness distribution of transverse shear stress ($\bar{\tau}_{zy}$) of orthotropic plate for aspect ratio 4 using equations of equilibrium

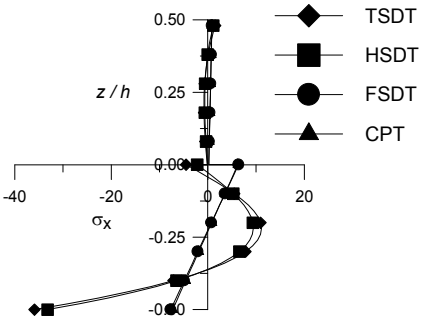


Fig. 5 Through thickness distribution of inplane normal stress ($\bar{\sigma}_x$) in ($0^0/90^0$) laminated plate for aspect ratio 4

https://doi.org/10.1017/jmech.2012.131 Published online by Cambridge University Press

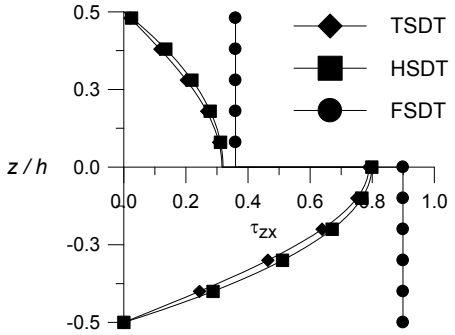


Fig. 6 Through thickness distribution of transverse shear stress ($\bar{\tau}_{zx}$) of ($0^0/90^0$) laminated plate for aspect ratio 4 using constitutive relations

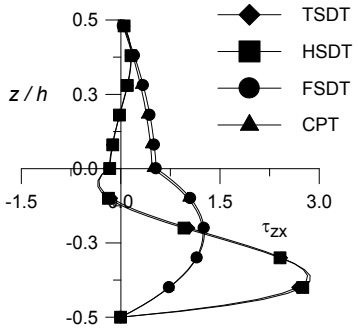


Fig. 7 Through thickness distribution of transverse shear stress ($\bar{\tau}_{zx}$) in ($0^0/90^0$) laminated plate for aspect ratio 4 using equations of equilibrium

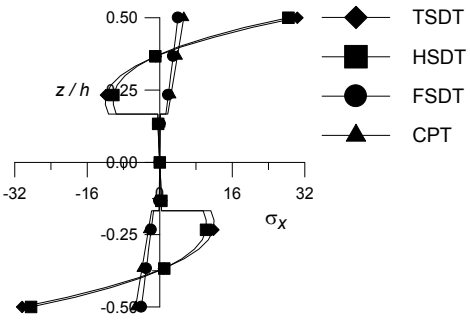


Fig. 8 Through thickness distribution of inplane normal stress ($\bar{\sigma}_x$) in ($0^0/90^0/0^0$) laminated plate for aspect ratio 4

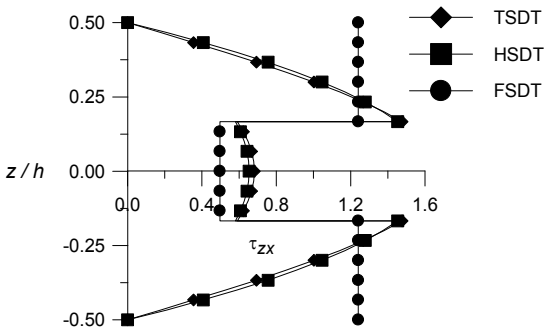


Fig. 9 Through thickness distribution of transverse shear stress ($\bar{\tau}_{zx}$) in ($0^0/90^0/0^0$) laminated plate for aspect ratio 4 using constitutive relations

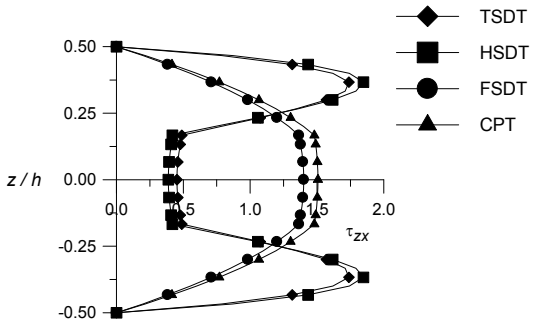


Fig. 10 Through thickness distribution of transverse shear stress ($\bar{\tau}_{zx}$) of ($0^0/90^0/0^0$) laminated plate for aspect ratio 4 using equations of equilibriums

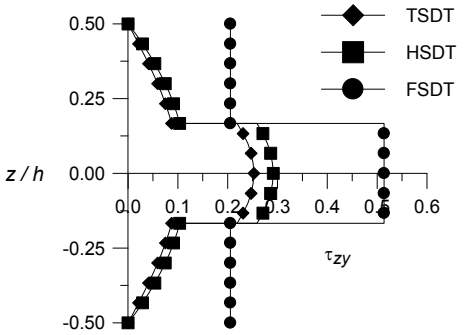


Fig. 11 Through thickness distribution of transverse shear stress ($\bar{\tau}_{zy}$) of ($0^0/90^0/0^0$) laminated plate for aspect ratio 4 using constitutive relations

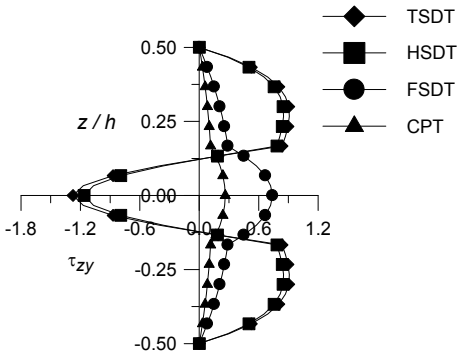


Fig. 12 Through thickness distribution of transverse shear stress ($\bar{\tau}_{zy}$) of ($0^0/90^0/0^0$) laminated plate for aspect ratio 4 using equations of equilibrium

to heavy stress concentration. Through thickness distribution of inplane normal stress $\bar{\sigma}_y$ is similar to distribution of $\bar{\sigma}_x$ with maximum value at $z = h/2$ and minimum value at $z = -h/2$. The maximum values of inplane normal stresses $\bar{\sigma}_x$ and $\bar{\sigma}_y$ for three layered symmetric laminated plates are shown in Table 7 and distribution of $\bar{\sigma}_x$ is shown in Fig. 8. The inplane normal stress $\bar{\sigma}_x$ is maximum in 0^0 layers ($z = -h/2$ to $z = -h/6$ and $z = h/6$ to $z = h/2$) and minimum in 90^0 layer ($z = -h/6$ to $z = h/6$).

https://doi.org/10.1017/jmech.2012.131 Published online by Cambridge University Press

Table 1 Comparison of maximum inplane normal stresses $\bar{\sigma}_x$ and $\bar{\sigma}_y$ at ($x = a / 2, y = b / 2, z = \pm h / 2$) in square orthotropic plate subjected to central concentrated load

S	Theory	Model	$\bar{\sigma}_x$	$\bar{\sigma}_y$
4	Present	TSDT	33.342	5.364
	Reddy [10]	HSDT	29.800	4.115
	Mindlin [5]	FSDT	4.8622	1.231
	Kirchhoff [1,2]	CPT	5.8047	0.826
10	Present	TSDT	18.433	2.514
	Reddy [10]	HSDT	15.911	1.975
	Mindlin [5]	FSDT	5.1953	1.076
	Kirchhoff [1,2]	CPT	5.8047	0.826

Table 2 Comparison of maximum transverse shear stress $\bar{\tau}_{zx}$ at ($x = 0, y = b / 2, z$) in square orthotropic plate subjected to central concentrated load

S	Theory	Model	$\bar{\tau}_{zx}^{CR}$	$\bar{\tau}_{zx}^{EE}$
4	Present	TSDT	1.4395	1.8858
	Reddy [10]	HSDT	1.4204	1.9827
	Mindlin [5]	FSDT	1.2082	1.8124
	Kirchhoff [1,2]	CPT	–	1.8144
10	Present	TSDT	1.5057	2.0021
	Reddy [10]	HSDT	1.5280	1.9025
	Mindlin [5]	FSDT	1.2393	1.8590
	Kirchhoff [1,2]	CPT	–	1.8144

Table 3 Comparison of maximum transverse shear stress $\bar{\tau}_{zy}$ at ($x = 0, y = b / 2, z$) in square orthotropic plate subjected to central concentrated load

S	Theory	Model	$\bar{\tau}_{zy}^{CR}$	$\bar{\tau}_{zy}^{EE}$
4	Present	TSDT	0.0599	0.6893
	Reddy [10]	HSDT	0.0627	0.6024
	Mindlin [5]	FSDT	0.2024	0.3037
	Kirchhoff [1,2]	CPT	–	0.1338
10	Present	TSDT	0.0844	0.4558
	Reddy [10]	HSDT	0.0901	0.3134
	Mindlin [5]	FSDT	0.1428	0.2142
	Kirchhoff [1,2]	CPT	–	0.1338

Table 4 Comparison of maximum inplane normal stress $\bar{\sigma}_x$ and $\bar{\sigma}_y$ at ($x = a / 2, y = b / 2, z$) in square ($0^0/90^0$) laminated plate subjected to central concentrated load

S	Theory	Model	$\bar{\sigma}_x$	$\bar{\sigma}_y$
4	Present	TSDT	35.905	35.905
	Reddy [10]	HSDT	33.183	33.183
	Mindlin [5]	FSDT	7.7032	7.7032
	Kirchhoff [1,2]	CPT	7.2859	7.2859
10	Present	TSDT	21.048	21.048
	Reddy [10]	HSDT	18.479	18.479
	Mindlin [5]	FSDT	7.5731	7.5731
	Kirchhoff [1,2]	CPT	7.2859	7.2859

Table 5 Comparison of maximum transverse shear stress $\bar{\tau}_{zx}$ at ($x = 0, y = b / 2, z$) in square ($0^0/90^0$) laminated plate subjected to central concentrated load

S	Theory	Model	$\bar{\tau}_{zx}^{CR}$	$\bar{\tau}_{zx}^{EE}$
4	Present	TSDT	0.7891	2.8245
	Reddy [10]	HSDT	0.7987	2.8615
	Mindlin [5]	FSDT	0.8994	1.2648
	Kirchhoff [1,2]	CPT	–	1.2438
10	Present	TSDT	0.7424	2.6929
	Reddy [10]	HSDT	0.8406	2.3644
	Mindlin [5]	FSDT	0.8351	1.1946
	Kirchhoff [1,2]	CPT	–	1.2438

Table 6 Comparison of maximum transverse shear stress $\bar{\tau}_{zy}$ at ($x = a / 2, y = 0, z$) in square ($0^0/90^0$) laminated plate subjected to central concentrated load

S	Theory	Model	$\bar{\tau}_{zy}^{CR}$	$\bar{\tau}_{zy}^{EE}$
4	Present	TSDT	0.7891	2.8245
	Reddy [10]	HSDT	0.7987	2.8615
	Mindlin [5]	FSDT	0.8994	1.2648
	Kirchhoff [1,2]	CPT	–	1.2438
10	Present	TSDT	0.7424	2.6929
	Reddy [10]	HSDT	0.8406	2.3644
	Mindlin [5]	FSDT	0.8351	1.1946
	Kirchhoff [1,2]	CPT	–	1.2438

Table 7 Comparison of maximum inplane normal stress $\bar{\sigma}_x$ at ($x = a / 2, y = b / 2, z = \pm h / 2$) in square ($0^0/90^0/0^0$) laminated plate subjected to central concentrated load

S	Theory	Model	$\bar{\sigma}_x$	$\bar{\sigma}_y$
4	Present	TSDT	30.367	4.971
	Reddy [10]	HSDT	28.381	3.895
	Mindlin [5]	FSDT	4.0491	0.982
	Kirchhoff [1,2]	CPT	5.3352	0.581
10	Present	TSDT	17.655	2.498
	Reddy [10]	HSDT	15.715	1.859
	Mindlin [5]	FSDT	4.5169	0.823
	Kirchhoff [1,2]	CPT	5.3352	0.581

Table 8 Comparison of maximum transverse shear stress $\bar{\tau}_{zx}$ at ($x = 0, y = b / 2, z$) in square ($0^0/90^0/0^0$) laminated plate subjected to central concentrated load

S	Theory	Model	$\bar{\tau}_{zx}^{CR}$	$\bar{\tau}_{zx}^{EE}$
4	Present	TSDT	0.6821	1.7390
	Reddy [10]	HSDT	0.6539	1.8473
	Mindlin [5]	FSDT	0.4967	1.4008
	Kirchhoff [1,2]	CPT	–	1.5072
10	Present	TSDT	0.8027	1.8924
	Reddy [10]	HSDT	0.7867	1.8212
	Mindlin [5]	FSDT	0.5378	1.5122
	Kirchhoff [1,2]	CPT	–	1.5072

https://doi.org/10.1017/jmech.2012.131 Published online by Cambridge University Press

Table 9 Comparison of maximum transverse shear stress $\bar{\tau}_{zy}$ at ($x = a / 2$, $y = 0$, z) in square ($0^0/90^0/0^0$) laminated plate subjected to center concentrated load

S	Theory	Model	$\bar{\tau}_{zy}^{CR}$	$\bar{\tau}_{zy}^{EE}$
4	Present	TSDT	0.2527	1.2756
	Reddy [10]	HSDT	0.2915	1.1628
	Mindlin [5]	FSDT	0.5140	0.7392
	Kirchhoff [1,2]	CPT	–	0.2620
10	Present	TSDT	0.1654	0.6871
	Reddy [10]	HSDT	0.1701	0.6312
	Mindlin [5]	FSDT	0.3140	0.4563
	Kirchhoff [1,2]	CPT	–	0.2620

2. Transverse Shear Stresses ($\bar{\tau}_{zx}$ and $\bar{\tau}_{yz}$):

The transverse shear stresses are obtained by using constitutive relations and, alternatively, by integration of equation of equilibrium of theory of elasticity and are denoted by ($\bar{\tau}_{zx}^{CR}$, $\bar{\tau}_{zy}^{CR}$) and ($\bar{\tau}_{zx}^{EE}$, $\bar{\tau}_{zx}^{EE}$) respectively. The transverse shear stresses satisfies the stress free conditions on the top ($z = -h/2$) and bottom ($z = h/2$) surfaces of the plate when these stresses are obtained by both mentioned approaches. The comparison of maximum non-dimensional transverse shear stresses for orthotropic plate, obtained by present theory and other refined theories is presented in Tables 2 and 3. The results obtained by present theory and HSDT are in close agreement with each other whereas FSDT and CPT underestimates the same when obtained by using constitutive relations as well as equation of equilibrium. Figures 3 and 4 contains the through thickness distribution of transverse shear stresses $\bar{\tau}_{zx}$ and $\bar{\tau}_{zy}$ respectively obtained by using equations of equilibrium. It is observed that these distributions deviates more from those given by FSDT and CPT. The point of maximum shear is no longer at the neutral plane but it is moved towards extreme fibres. These distributions change their sign across the thickness of plate. At the neutral plane ($z = 0$) these gives maximum negative value and at $z = \pm 0.34h$ these gives maximum positive values. This anomalous behavior of these stresses is due to heavy local stress concentration because of central concentrated load.

The maximum values of transverse shear stresses $\bar{\tau}_{zx}$ and $\bar{\tau}_{zy}$ for two layered anti-symmetric ($0^0/90^0$) laminated plates are presented in Tables 5 and 6 are identical. Since the effect of stress concentration can not be assessed by constitutive relations, the results obtained from constitutive relation and equilibrium equations are quite different from each other in these Tables. Through thickness distributions of transverse shear stress $\bar{\tau}_{zx}$ are shown in Figs. 6 and 7. The stress variation shown in Fig. 6 is obtained by constitutive relation which gives a discontinuity of stresses at interface in case of laminated plates and also, these relations cannot assess the effect of stress concentration. The stress variation shown in Fig. 7 is obtained by equations of equilibrium. This stress distribution is positive throughout the thickness of plate when obtained using FSDT and CPT whereas it changes its sign in both the layers when obtained using present theory and HSDT due effect of stress concentration. At the neutral plane ($z = 0$) it gives maximum negative value and at $z = -0.36h$ it gives maximum positive value. Distribution of transverse shear stress $\bar{\tau}_{yz}$ follows the same trend with interchange in lamination configuration ($90^0/0^0$). The maximum values of transverse shear stresses for three layered symmetric laminated plates are presented in Tables 8 and 9 and their distribution through the thickness of plates are shown in Figs. 9 through 12.

CONCLUSIONS

In this paper effect of transverse shear deformation, transverse normal strain and local stress concentration on inplane normal and transverse shear stresses through the thickness of simply supported orthotropic and laminated plates is studied. Following conclusions are drawn from this investigation.

1. The through thickness distribution of inplane normal stresses is found to be non-linear and deviates considerably from classical plate theory and first order shear deformation theory.
2. The transverse shear stresses predicted by present theory and theory of Reddy are in close agreement when obtained using constitutive relations.
3. The distribution of transverse shear stresses is realistic but changes its sign when obtained using integration of equations of equilibrium.
4. Present theory seems to be capable of predicting the effect of heavy stress concentration more prominently compared to other theories.

APPENDIX

The elements of stiffness matrix appeared in Eq. (63) are as follows:

$$K_{11} = (A_{11}\alpha^2 + A_{66}\beta^2)\ ;$$

$$K_{12} = (A_{12} + A_{66})\alpha\beta\ ;$$

$$K_{13} = -B_{11}\alpha^3 - (B_{12} + 2B_{66})\alpha\beta^2\ ;$$

$$K_{14} = (As_{11}\alpha^2 + As_{66}\beta^2)\ ;$$

$$K_{15} = (As_{12} + As_{66})\alpha\beta\ ;$$

$$K_{16} = \frac{\pi}{h} As_{13}\alpha\ ;$$

https://doi.org/10.1017/jmech.2012.131 Published online by Cambridge University Press

$$K_{22} = (A_{66}\,\alpha^2 + A_{22}\,\beta^2)\ ;$$

$$K_{23} = -B_{22}\,\beta^3 - (B_{12} + 2B_{66})\alpha^2\,\beta\ ;$$

$$K_{24} = (As_{12} + As_{66})\,\alpha\,\beta\ ;$$

$$K_{25} = (As_{66}\,\alpha^2 + As_{22}\,\beta^2)\ ;$$

$$K_{26} = \frac{\pi}{h} As_{23}\ \beta\ ;$$

$$K_{33} = D_{11}\alpha^4 + 2(D_{12} + 2D_{66})\ \alpha^2\beta^2 + D_{22}\beta^4\ ;$$

$$K_{34} = -Bs_{11}\,\alpha^3 - (Bs_{12} + 2Bs_{66})\ \alpha\beta^2\ ;$$

$$K_{35} = -Bs_{22}\,\beta^3 - (Bs_{12} + 2Bs_{66})\ \alpha^2\,\beta\ ;$$

$$K_{36} = \frac{\pi}{h}(Bs_{13}\,\alpha^2 + Bs_{23}\,\beta^2)\ ;$$

$$K_{44} = (Ass_{11}\,\alpha^2 + Ass_{66}\,\beta^2 + Acc_{55})\ ;$$

$$K_{45} = (Ass_{12} + Ass_{66})\,\alpha\,\beta\ ;$$

$$K_{46} = \left(\frac{\pi}{h} Ass_{13} + \frac{h}{\pi} Acc_{55}\right)\alpha\ ;$$

$$K_{55} = (Ass_{66}\,\alpha^2 + Ass_{22}\,\beta^2 + Acc_{44})\ ;$$

$$K_{56} = \left(\frac{\pi}{h} Ass_{23} + \frac{h}{\pi} Acc_{44}\right)\beta\ ;$$

$$K_{66} = \left(\frac{h^2}{\pi^2} Acc_{55}\,\alpha^2 + \frac{h^2}{\pi^2} Acc_{44}\,\beta^2 + \frac{\pi^2}{h^2} Ass_{33}\right)\ .$$

where, constants A_{ij}, B_{ij}, D_{ij}, As_{ij}, Bs_{ij}, Ass_{ij} and Acc_{ij} are defined as follows:

$$\begin{bmatrix} A_{ij} \\ B_{ij} \\ D_{ij} \end{bmatrix} = \bar{Q}_{ij}^k \int_{-h/2}^{h/2} \begin{bmatrix} 1 \\ z \\ z^2 \end{bmatrix} dz \quad (i, j = 1, 2, 6)\ ,$$

$$\begin{bmatrix} As_{ij} \\ Bs_{ij} \\ Ass_{ij} \end{bmatrix} = \bar{Q}_{ij}^k \int_{-h/2}^{h/2} \begin{bmatrix} f(z) \\ z\ f(z) \\ [f(z)]^2 \end{bmatrix} dz \ \ (i, j = 1,\ 2,\ 6)\ ,$$

$$Acc_{ij} = \bar{Q}_{ij}^k \int_{-h/2}^{h/2} [f'(z)]^2\, dz \ \ (i, j = 4,\ 5)$$

The constants $\bar{u}, \bar{v}, \bar{w}, \bar{\phi}, \bar{\psi}$ and $\bar{\xi}$ appeared in Eq. (64) are given below:

$$\bar{u} = -\left(\frac{K_{12}}{K_{11}}\bar{v} + \frac{K_{13}}{K_{11}}\bar{w} + \frac{K_{14}}{K_{11}}\bar{\phi} + \frac{K_{15}}{K_{11}}\bar{\psi} + \frac{K_{16}}{K_{11}}\bar{\xi}\right)\ ;$$

$$\bar{v} = -\left(\frac{x_2}{x_1}\bar{w} + \frac{x_3}{x_1}\bar{\phi} + \frac{x_4}{x_1}\bar{\psi} + \frac{x_5}{x_1}\bar{\xi}\right)\ ;$$

$$\bar{w} = \left(\frac{1}{y_1} - \frac{y_2}{y_1}\bar{\phi} + \frac{y_3}{y_1}\bar{\psi} + \frac{y_4}{y_1}\bar{\xi}\right)\ ;$$

$$\bar{\phi} = -\left(\frac{R_1}{R_2} + \frac{R_3}{R_2}\bar{\psi} + \frac{R_4}{R_2}\bar{\xi}\right)\ ;$$

$$\bar{\psi} = \left(\frac{P_3\, z_1}{P_2\, z_2} - \frac{P_1}{P_2}\right) \text{ and } \bar{\xi} = \left(-\frac{z_1}{z_2}\right)$$

where

$$x_1 = \left(K_{22} - \frac{K_{12}K_{12}}{K_{11}}\right)\ ;\ x_2 = \left(K_{23} - \frac{K_{12}K_{13}}{K_{11}}\right)\ ;$$

$$x_3 = \left(K_{24} - \frac{K_{12}K_{14}}{K_{11}}\right)\ ;\ x_4 = \left(K_{25} - \frac{K_{12}K_{15}}{K_{11}}\right)\ ;$$

$$x_5 = \left(K_{26} - \frac{K_{12}K_{16}}{K_{11}}\right)\ ;\ x_6 = \left(K_{23} - \frac{K_{13}K_{12}}{K_{11}}\right)\ ;$$

$$x_7 = \left(K_{33} - \frac{K_{13}K_{13}}{K_{11}}\right)\ ;\ x_8 = \left(K_{34} - \frac{K_{13}K_{14}}{K_{11}}\right)\ ;$$

$$x_9 = \left(K_{35} - \frac{K_{13}K_{15}}{K_{11}}\right)\ ;\ x_{10} = \left(K_{36} - \frac{K_{13}K_{16}}{K_{11}}\right)\ ;$$

$$x_{11} = \left(K_{24} - \frac{K_{14}K_{12}}{K_{11}}\right)\ ;\ x_{12} = \left(K_{34} - \frac{K_{14}K_{13}}{K_{11}}\right)\ ;$$

$$x_{13} = \left(K_{44} - \frac{K_{14}K_{14}}{K_{11}}\right)\ ;\ x_{14} = \left(K_{45} - \frac{K_{14}K_{15}}{K_{11}}\right)\ ;$$

$$x_{15} = \left(K_{46} - \frac{K_{14}K_{16}}{K_{11}}\right)\ ;\ x_{16} = \left(K_{25} - \frac{K_{15}K_{12}}{K_{11}}\right)\ ;$$

$$x_{17} = \left(K_{35} - \frac{K_{15}K_{13}}{K_{11}}\right)\ ;\ x_{18} = \left(K_{45} - \frac{K_{15}K_{14}}{K_{11}}\right)\ ;$$

$$x_{19} = \left(K_{55} - \frac{K_{15}K_{15}}{K_{11}}\right)\ ;\ x_{20} = \left(K_{56} - \frac{K_{15}K_{16}}{K_{11}}\right)\ ;$$

$$x_{21} = \left(K_{26} - \frac{K_{16}K_{12}}{K_{11}}\right)\ ;\ x_{22} = \left(K_{36} - \frac{K_{16}K_{13}}{K_{11}}\right)\ ;$$

$$x_{23} = \left(K_{46} - \frac{K_{16}K_{14}}{K_{11}}\right)\ ;\ x_{24} = \left(K_{56} - \frac{K_{16}K_{15}}{K_{11}}\right)\ ;$$

$$x_{25} = \left(K_{66} - \frac{K_{16}K_{16}}{K_{11}}\right)\ ;$$

$$y_1 = \left(x_7 - \frac{x_6\, x_2}{x_1}\right)\ ;\ y_2 = \left(x_8 - \frac{x_6\, x_3}{x_1}\right)\ ;$$

$$y_3 = \left(x_9 - \frac{x_6\, x_4}{x_1}\right)\ ;\ y_4 = \left(x_{10} - \frac{x_6\, x_5}{x_1}\right)\ ;$$

$$y_5 = \left(x_{12} - \frac{x_{11}\, x_2}{x_1}\right)\ ;\ y_6 = \left(x_{13} - \frac{x_{11}\, x_2}{x_1}\right)\ ;$$

$$y_7 = \left(x_{14} - \frac{x_{11}\, x_2}{x_1}\right)\ ;\ y_8 = \left(x_{15} - \frac{x_{11}\, x_2}{x_1}\right)\ ;$$

$$y_9 = \left(x_{17} - \frac{x_{16}\, x_2}{x_1}\right)\ ;\ y_{10} = \left(x_{18} - \frac{x_{16}\, x_2}{x_1}\right)\ ;$$

$$y_{11} = \left(x_{19} - \frac{x_{16}\, x_2}{x_1}\right)\ ;\ y_{12} = \left(x_{20} - \frac{x_{16}\, x_2}{x_1}\right)\ ;$$

$$y_{13} = \left(x_{22} - \frac{x_{21}\, x_2}{x_1}\right)\ ;\ y_{14} = \left(x_{23} - \frac{x_{21}\, x_2}{x_1}\right)\ ;$$

$$y_{15} = \left(x_{24} - \frac{x_{21}\, x_2}{x_1}\right)\ ;\ y_{16} = \left(x_{25} - \frac{x_{21}\, x_2}{x_1}\right)\ ;$$

https://doi.org/10.1017/jmech.2012.131 Published online by Cambridge University Press

$$R_1 = \left(\frac{y_5}{y_1}\right);\quad R_2 = \left(y_6 - \frac{y_5\, y_2}{y_1}\right);\quad R_3 = \left(y_7 - \frac{y_5\, y_3}{y_1}\right);$$

$$R_4 = \left(y_8 - \frac{y_5\, y_4}{y_1}\right);\quad R_5 = \left(\frac{y_9}{y_1}\right);\quad R_6 = \left(y_{10} - \frac{y_9\, y_2}{y_1}\right);$$

$$R_7 = \left(y_{11} - \frac{y_9\, y_3}{y_1}\right);\quad R_8 = \left(y_{12} - \frac{y_9\, y_4}{y_1}\right);\quad R_9 = \left(\frac{y_{13}}{y_1}\right);$$

$$R_{10} = \left(y_{14} - \frac{y_{13}\, y_2}{y_1}\right);\quad R_{11} = \left(y_{15} - \frac{y_{13}\, y_3}{y_1}\right);$$

$$R_{12} = \left(y_{16} - \frac{y_{13}\, y_4}{y_1}\right);$$

$$P_1 = \left(R_5 - \frac{R_6\, R_1}{R_2}\right);\quad P_2 = \left(R_7 - \frac{R_6\, R_3}{R_2}\right);$$

$$P_3 = \left(R_8 - \frac{R_6\, R_4}{R_2}\right);\quad P_4 = \left(R_9 - \frac{R_{10}\, R_1}{R_2}\right);$$

$$P_5 = \left(R_{11} - \frac{R_{10}\, R_3}{R_2}\right);\quad P_6 = \left(R_{12} - \frac{R_{10}\, R_4}{R_2}\right);$$

$$z_1 = \left(P_4 - \frac{P_5\, P_1}{P_2}\right);\quad z_2 = \left(P_6 - \frac{P_5\, P_3}{P_2}\right)$$

REFERENCES

1. Kirchhoff, G. R., "Uber Das Gleichgewicht Und Die Bewegung Einer Elastischen Scheibe," *Journal fur die Reine und Angewandte Mathematik (Crelle) [Journal for Pure and Applied Mathematics]*, **40**, pp. 51–88 (1850).
2. Kirchhoff, G. R., "Uber Die Uchwingungen Einer Kriesformigen Elastischen Scheibe," *Poggendorffs Annalen*, **81**, pp. 58–264 (1850).
3. Reissner, E., "On the Theory of Bending of Elastic Plates," *Journal of Mathematics and Physics*, **23**, pp. 184–191 (1944).
4. Reissner, E., "The Effect of Transverse Shear Deformation on the Bending of Elastic Plates," *Journal of Applied Mechanics*, ASME, **12**, pp. 69–77 (1945).
5. Mindlin, R. D., "Influence of Rotatory Inertia and Shear on Flexural Motions of Isotropic, Elastic Plates," *Journal of Applied Mechanics*, ASME, **18**, pp. 31–38 (1951).
6. Lo, K. H., Christensen, R. M. and Wu, E. M., "A High-Order Theory of Plate Deformation, Part-1: Homogeneous Plates," *Journal of Applied Mechanics*, ASME, **44**, pp. 663–668 (1977).
7. Lo, K. H., Christensen, R. M. and Wu, E. M., "A High-Order Theory of Plate Deformation, Part-2: Laminated Plates," *Journal of Applied Mechanics*, ASME, **44**, pp. 669–676 (1977).
8. Lo, K. H., Christensen, R. M. and Wu, E. M., "Stress Solution Determination for Higher Order Plate Theory," *Journal of Solids and Structures*, **14**, pp. 655–662 (1978).
9. Reddy, J. N., "A Refined Nonlinear Theory of Plates with Transverse Shear Deformation," *Journal of Solids and Structures*, **20**, pp. 881–896 (1984).
10. Reddy, J. N., "A Simple Higher Order Theory for Laminated Composite Plates," *Journal of Applied Mechanics*, ASME, **51**, pp. 745–752 (1978).
11. Kant, T., "Numerical Analysis of Thick Plates," *Computer Methods in Applied Mechanics and Engineering*, **31**, pp. 1–18 (1978).
12. Savithri, S. and Varadan, T. K., "A Simple Higher Order Theory for Homogenous Plates," *Mechanics Research Communications*, **19**, pp. 65–71 (1992).
13. Noor, A. K. and Burton, W. S., "Assessment of Shear Deformation Theories for Multilayered Composite Plates," *Applied Mechanics Reviews*, **42**, pp. 1–13 (1989).
14. Ghugal, Y. M. and Shimpi, R. P., "A Review of Refined Shear Deformation Theories for Isotropic and Anisotropic Laminated Plates," *Journal of Reinforced Plastics and Composites*, **21**, pp. 775–813 (2002).
15. Levy, M., "Memoire Dur La Theorie Des Plaques Elastique Planes," *Journal of Des Mathematiques Pures et Appliquees*, **30**, pp. 219–306 (1877).
16. Stein, M., "Nonlinear Theory for Plates and Shells Including Effect of Shearing," *AIAA Journal*, **24**, pp. 1537–1544 (1986).
17. Stein, M. and Bains, N. J. C., "Post Buckling Behavior of Longitudinally Compressed Orthotropic Plates with Transverse Shearing Flexibility," *AIAA Journal*, **28**, pp. 892–895 (1990).
18. Stein, M. and Jegly, D. C., "Effect of Transverse Shearing on Cylindrical Bending, Vibration and Buckling of Laminate Plates," *AIAA Journal*, **25**, pp. 123–129 (1987).
19. Liu, D. and Li, X., "An Overall View of Laminate Theories Based on Displacement Hypothesis," *Journal of Composite Materials*, **30**, pp. 1539–1561 (1996).
20. Reddy, J. N. and Robbins, D. H. Jr., "Theories and Computational Models for Composite Laminates," *Applied Mechanics Reviews*, **47**, pp. 147–169 (1994).
21. Manjunatha, B. S. and Kant, T., "Different Numerical Techniques for the Estimation of Multiaxial Stresses in Symmetric/Unsymmetric Composite and Sandwich Beams with Refined Theories," *Journal of Reinforced Plastics and Composites*, **12**, pp. 2–37 (1993).
22. Vinayak, R. U., Prathap, G. and Naganarayana, B. P., "Beam Elements Based on a Higher Order Theory — I: Formulation and Analysis of Performance," *Computers and Structures*, **58**, pp. 775–789 (1996).
23. Jones, R. M., *Mechanics of Composite Materials*, McGraw Hill Kogakusha, Ltd, Tokyo (1975).
24. Pagano, N. J., "Exact Solutions for Bidirectional Composites and Sandwich Plates," *Journal of Composite Materials*, **4**, pp. 20–34 (1970).

(Manuscript received December 5, 2011, accepted for publication July 30, 2012.)

https://doi.org/10.1017/jmech.2012.131 Published online by Cambridge University Press